Adaptive Carrier Synchronization Using Decision-Aided Kalman Filtering Algorithms

Wei-Tsen Lin and Dah-Chung Chang, *Member*, IEEE

Abstract —*A new adaptive carrier recovery algorithm is proposed by using the decision-aided extended Kalman filtering technique. In order to reduce computational complexity of the Kalman recursions, the state model in the new algorithm uses only phase rather than both phase and frequency which are usually used in conventional modeling. The frequency is considered as an input term to the system equation and estimated by a phase error detector. A reduced observation model is also introduced to relieve computing load from multiple matrix to scalar operations in the Kalman recursions. Simulations show that the proposed one-state Kalman algorithm has better performance and lower complexity than the two-state Kalman algorithm for synchronization applications. The new algorithm is applied to the cable modem downstream system to demonstrate its effectiveness with FPGA implementation results.*

Index Terms— Extended Kalman filter, state model, carrier synchronization, downstream, FPGA.

I. INTRODUCTION

CARRIER synchronization is an important part in coherent communication systems, especially for those employing a high bandwidth-efficient modulation scheme such as quadrature amplitude modulation (QAM) [1, 2]. Carrier frequency offset is usually inevitable because of the frequency mismatch of local oscillators between the transmitter and the receiver. Moreover, the Doppler effect due to the mobile communication environment is also an influential factor. Not only is carrier synchronization important in conventional single-carrier communication systems, but also is necessary in multicarrier communication systems [3, 15, 16].

A traditional method to implement the carrier recovery system is to use the phase-locked loop (PLL) [4-10] technique in the receiver. Despite its simplicity and feasibility, the PLL indeed suffers from a major drawback that requires the trade-off between fast acquisition and small steady-state phase tracking variation due to a fixed loop bandwidth. A larger loop bandwidth usually results in faster acquisition and considerable steady-state phase tracking variation while a smaller loop bandwidth can reach a better steady-state performance with a long acquisition time. Some researches about PLL focused on the design of phase or frequency error detectors [6-8]. In practice, it is a problem to determine appropriate parameters for the loop filter in a stringent environment. From the theoretical point of view, faster acquisition and smaller steady-state phase tracking variation might be simultaneously considered by changing the loop bandwidth through a variety of parameter setup stages in the convergence process.

Studies aimed at achieving fast convergence rate while reducing the steady-state phase tracking variation can be found in the literature [9-16]. Some of them modify the original PLL structure such as [9-10], other alternatives use Kalman filter algorithms [11-16]. In [9] the loop bandwidth is adjusted by certain control mechanisms following the status of the frequency estimate proposed in [10]. Such a method can be generally regarded as a multi-stage approach with a set of pre-defined parameters. The Kalman filter is known as the optimally recursive linear filter in the minimum mean squared error (MMSE) sense [17]. The modeling approach in [11, 12] incorporates the phase and frequency variables into the system model. Since the relationship of phase and observations can be nonlinear in the measurement equation and thus the extended Kalman filter [17] is applied.

The conventional PLL method is concerned with a tradeoff between performance and convergence rate and this motivates the use of an adaptive loop bandwidth to obtain better results. By modeling the carrier drift as a Kalman filtering problem, not only the loop bandwidth can be adaptively adjusted but also the loop filter parameters are further simplified to the setup of process and measurement noise variances. Besides, whenever the system environment varies, the Kalman filter can adaptively cope with such changes better than a traditional PLL can do.

In this paper, we propose a new adaptive carrier synchronization technique applying the extended Kalman filtering algorithm. The main idea in the proposed scheme is the state and observation reduction to relieve computing load from multiple matrix to scalar operations compared to the conventional two-state modeling. Although some researches [13, 14] as well used only phase in the Kalman recursions, the phase was modeled as a Wiener process that did not efficiently express the phase as a relation to the frequency. In order to improve the performance of carrier frequency estimation, the frequency is modeled as an input term to the system equation and is estimated by a phase error detector. We also study the performance of a reduced observation model with only the in-phase or the quadrature component used for the measurement equation. The proposed method is applied to a practical example of the cable modem downstream receiver

This work was supported in part by the National Science Council of Taiwan under the contract 95-2220-E-008-003.

Wei-Tsen Lin is with MediaTek Inc., No. 1, Dusing Rd. 1, Science-Based Industrial Park, Hsinchu City, Taiwan 300.

Dah-Chung Chang is with Department of Communication Engineering, National Central University, N300 Jhongda Rd., JhongLi City, Taoyuang, 320, Taiwan. (e-mail: dcchang@ce.ncu.edu.tw).

Contributed Paper
Original manuscript received July 22, 2007
Revised manuscript received August 16, 2007

with blind channel equalization [1, 2]. In addition to the algorithm-level simulation results, the implementation results on Xilinx Spartan-3 FPGA are demonstrated to show the effectiveness of this new carrier recovery loop.

II. The Extended Kalman Filtering algorithm

The state variable in an extended Kalman filter (EKF) relates to the state dynamics and the measurements by the following state equation and measurement equation:

$$\begin{cases} x_{k+1} = f_k(x_k) + g_k(x_k)w_k & (1) \\ z_k = h_k(x_k) + v_k & (2) \end{cases}$$

where x_k denotes the state vector that may contain many parameters to be estimated, the subscript k is the discrete-time sample index, z_k contain observations, the functions $f_k(\cdot)$ and $h_k(\cdot)$ are nonlinear dynamic and measurement equations in discrete-time modeling, respectively, and w_k and v_k are process and measurement noises, respectively. The nonlinear models can be approximated to linear equations that conform to the Kalman filtering algorithm by Taylor expansion. The linearized result can be thought as a suboptimal algorithm in MMSE sense to the estimation of x_k even though the variables x_k, w_k, and v_k are mutually uncorrelated and white Gaussian processes. The extended Kalman filtering algorithm is summarized in Table I.

III. EKF for Adpative Carrier Recovery

A. The Two-State Modeling Approach

An approach to formulating the problem of carrier synchronization as a Kalman filtering problem as shown in Fig. 1 can be described by the following equations:

$$\begin{bmatrix} \theta_{k+1} \\ \omega_{k+1} \end{bmatrix} = \begin{bmatrix} 1 & 1 \\ 0 & 1 \end{bmatrix} \begin{bmatrix} \theta_k \\ \omega_k \end{bmatrix} + \begin{bmatrix} w_k^{\theta} \\ w_k^{\omega} \end{bmatrix} \quad (3)$$

$$z_k = \begin{bmatrix} z_k^I \\ z_k^Q \end{bmatrix} = \begin{bmatrix} u_k^I & -u_k^Q \\ u_k^Q & u_k^I \end{bmatrix} \begin{bmatrix} \cos\theta_k \\ \sin\theta_k \end{bmatrix} + \begin{bmatrix} v_k^I \\ v_k^Q \end{bmatrix} \quad (4)$$

where θ_k and ω_k are two parameters denoting the phase and frequency offset at the kth time instant, and w_k^{θ} and w_k^{ω} are the AWGN processes representing the modeling inaccuracy of the underlying system. u_k^I and u_k^Q are the transmitted in-phase (I) and quadrature (Q) components. The system observations z_k^I and z_k^Q are the I and Q components of the output signals with a carrier mismatch between the transmitter and the receiver. v_k^I and v_k^Q are the measurement AWGN with respect to the I and Q components, respectively.

TABLE I. The Extended Kalman Filtering Algorithm

SIGNAL MODEL (NONLINEAR):

$x_{k+1} = f_k(x_k) + g_k(x_k)w_k$, $z_k = h_k(x_k) + v_k$

SIGNAL MODEL (APPROXIMATE):

$x_{k+1} = F_k x_k + G_k w_k + u_k$, $z_k = H_k' x_k + v_k + y_k$

where $u_k = f_k(\hat{x}_{k/k}) - F_k \hat{x}_{k/k}$ and $y_k = h_k(\hat{x}_{k/k-1}) - H_k' \hat{x}_{k/k-1}$

$F_k = \frac{\partial f_k(x)}{\partial x}\Big|x = \hat{x}_{k/k}$, $H_k' = \frac{\partial h_k(x)}{\partial x}\Big|x = \hat{x}_{k/k-1}$, $G_k = g_k(\hat{x}_{k/k})$

ASSUMPTIONS:

x_0, $\{v_k\}$, $\{w_k\}$ are mutually independent; x_0 is $N(\bar{x}_0, P_0)$,

$\{v_k\}$ is zero mean, covariance $E\{v_k v_l'\} = R_k \delta_{kl}$; $\{w_k\}$ is zero mean,

covariance $E\{w_k w_l'\} = Q_k \delta_{kl}$

THE EXTENDED KALMAN FILTER RECURSIONS:

$\hat{x}_{k/k} = \hat{x}_{k/k-1} + L_k[z_k - h_k(\hat{x}_{k/k-1})]$, $\hat{x}_{k+1/k} = f_k(\hat{x}_{k/k})$

$\Omega_k = H_k' \Sigma_{k/k-1} H_k + R_k$

$L_k = \Sigma_{k/k-1} H_k \Omega_k^{-1}$

$\Sigma_{k/k} = \Sigma_{k/k-1} - \Sigma_{k/k-1} H_k \Omega_k^{-1} H_k' \Sigma_{k/k-1}$

$\Sigma_{k+1/k} = F_k \Sigma_{k/k} F_k' + G_k Q_k G_k'$

Initialization: $\Sigma_{0/-1} = P_0$, $\hat{x}_{0/-1} = \bar{x}_0$

NOTATION:

x_k, $\{x_k\}$:System state at time k and stochastic process formed by x_k

$\hat{x}_{k/k-1}$, $\hat{x}_{k/k}$: A-priori and a-posteriori state estimate

$\delta_{kl} = 1$ for $k = l$, otherwise 0; A' : Transpose of A

$N(\cdot)$: Gaussian distributed probability density function

$\Sigma_{k/k-1}$, $\Sigma_{k/k}$: A-priori and a-posteriori error covariance

By applying the extended Kalman filter algorithm to the system model depicted by (3) and (4), the state update equations can be obtained as

$$\begin{bmatrix} \hat{\theta}_{k/k} \\ \hat{\omega}_{k/k} \end{bmatrix} = \begin{bmatrix} \hat{\theta}_{k/k-1} \\ \hat{\omega}_{k/k-1} \end{bmatrix} + L_k \left\{ \begin{bmatrix} z_k^I \\ z_k^Q \end{bmatrix} - \begin{bmatrix} u_k^I & -u_k^Q \\ u_k^Q & u_k^I \end{bmatrix} \begin{bmatrix} \cos\hat{\theta}_{k/k-1} \\ \sin\hat{\theta}_{k/k-1} \end{bmatrix} \right\} \quad (5)$$

and

$$\begin{bmatrix} \hat{\theta}_{k+1/k} \\ \hat{\omega}_{k+1/k} \end{bmatrix} = \begin{bmatrix} 1 & 1 \\ 0 & 1 \end{bmatrix} \begin{bmatrix} \hat{\theta}_{k/k} \\ \hat{\omega}_{k/k} \end{bmatrix} \quad (6)$$

where L_k is the Kalman gain. The corresponding error covariance update equations are

$$\Sigma_{k/k} = \Sigma_{k/k-1} - \Sigma_{k/k-1} H_k \Omega_k^{-1} H_k' \Sigma_{k/k-1} \quad (7)$$

and

$$\Sigma_{k+1/k} = F_k \Sigma_{k/k} F_k' + G_k Q_k G_k' \quad (8)$$

where

$$F_k = \begin{bmatrix} 1 & 1 \\ 0 & 1 \end{bmatrix}, \; G_k = 1, \quad (9)$$

$$H_k' = \begin{bmatrix} -u_k^I \sin\hat{\theta}_{k/k-1} - u_k^Q \cos\hat{\theta}_{k/k-1} & 0 \\ -u_k^Q \sin\hat{\theta}_{k/k-1} + u_k^I \cos\hat{\theta}_{k/k-1} & 0 \end{bmatrix} \quad (10)$$

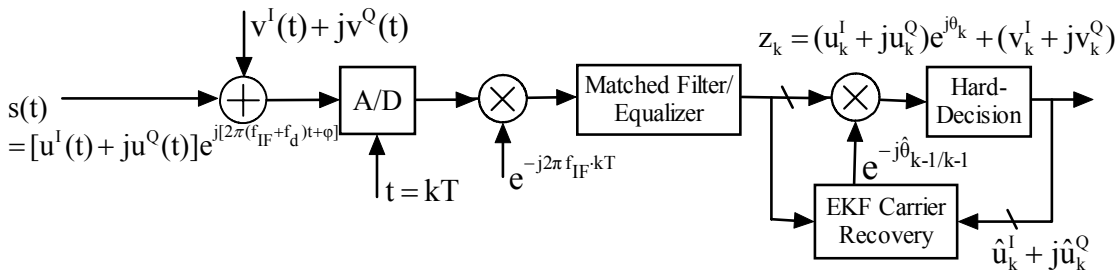

Fig. 1. The receiver carrier recovery system model.

In summary, the two-state Kalman filtering algorithm for adaptive carrier recovery consists of (5)-(10).

B. The Formulation of the One-State Modeling Approah

In the derivation of the preceding section, both the phase and frequency are two individual state parameters recursively updated by the Kalman filter. However, from the system perspective, the carrier frequency can be calculated as an external input. Based on this idea, the frequency in the state can be removed from the system model and consequently the computational requirement for the recursions can be reduced. The state model without frequency is then expressed as

$$\theta_{k+1}=\theta_k+\omega_k+w_k^\theta \tag{11}$$

The QAM constellation offset from its ideal position is caused by the frequency offset for each symbol. Let $\hat{u}_k^I$ and $\hat{u}_k^Q$ be the in-phase and the quadrature components of decision output signals, respectively. The following equation is used to estimate ω_k :

$$\hat{\omega}_k=\hat{\omega}_{k-1}+K_f\,\mathrm{Im}\left\{z_k e^{-j\hat{\theta}_{k/k-1}}(\hat{u}_k^I+j\hat{u}_k^Q)^*\right\} \tag{12}$$

where K_f is the step size controlling the convergence rate of the input estimation algorithm, **Im** denotes the imaginary part of the underlying argument; the term $z_k e^{-j\hat{\theta}_{k/k-1}}$ represents the signal rotating z_k with a phase angle $-\hat{\theta}_{k/k-1}$, $\hat{u}_k^I+j\hat{u}_k^Q$ is the kth transmitted data symbol obtained by the decision-aided data, and the symbol * takes the complex conjugate operation on its argument.

The Kalman filter equations using the one-state modeling approach are derived below. To update the state, it involves the following equations:

$$\hat{\theta}_{k/k}=\hat{\theta}_{k/k-1}+L_k\left\{\begin{bmatrix}z_k^I\\ z_k^Q\end{bmatrix}-\begin{bmatrix}u_k^I & -u_k^Q\\ u_k^Q & u_k^I\end{bmatrix}\begin{bmatrix}\cos\hat{\theta}_{k/k-1}\\ \sin\hat{\theta}_{k/k-1}\end{bmatrix}\right\} \tag{13}$$

$$\hat{\theta}_{k+1/k}=\hat{\theta}_{k/k}+\hat{\omega}_k \tag{14}$$

where L_k is the Kalman gain and the error covariance updates are the same as (7)-(8) except for some modifications in the following equations:

$$F_k=\left.\frac{\partial f_k(x)}{\partial x}\right|_{x=\hat{\theta}_{k/k}}=1, \tag{15}$$

$$G_k=g_k(\hat{\theta}_{k/k})=1, \tag{16}$$

$$H_k'=\left.\frac{\partial h_k(x)}{\partial x}\right|_{x=\hat{\theta}_{k/k-1}}=\begin{bmatrix}-u_k^I\sin\hat{\theta}_{k/k-1}-u_k^Q\cos\hat{\theta}_{k/k-1}\\ -u_k^Q\sin\hat{\theta}_{k/k-1}+u_k^I\cos\hat{\theta}_{k/k-1}\end{bmatrix} \tag{17}$$

Note that the calculation of H_k' needs the values of the transmitted symbol $u_k^I+ju_k^Q$ which is unknown at the receiver. Assume that the receiver works with a reasonably low error rate, then the decision-aided approach by taking the output of the hard-decision device as the transmitted symbol can be used. That is,

$$H_k'=\begin{bmatrix}-\hat{u}_k^I\sin\hat{\theta}_{k/k-1}-\hat{u}_k^Q\cos\hat{\theta}_{k/k-1}\\ -\hat{u}_k^Q\sin\hat{\theta}_{k/k-1}+\hat{u}_k^I\cos\hat{\theta}_{k/k-1}\end{bmatrix} \tag{18}$$

Thus, by replacing the transmitted symbol with the decision-aided data, the value of H_k' can be determined. Similarly, the state update in (13) can be rewritten as

$$\hat{\theta}_{k/k}=\hat{\theta}_{k/k-1}+L_k\left\{\begin{bmatrix}z_k^I\\ z_k^Q\end{bmatrix}-\begin{bmatrix}\hat{u}_k^I & -\hat{u}_k^Q\\ \hat{u}_k^Q & \hat{u}_k^I\end{bmatrix}\begin{bmatrix}\cos\hat{\theta}_{k/k-1}\\ \sin\hat{\theta}_{k/k-1}\end{bmatrix}\right\} \tag{19}$$

In conclusion, (7)-(8) and (14)-(19) form the one-state Kalman algorithm for adaptive carrier recovery.

C. The One-State Modeling with Reduced Observation

It is also possible to make the computational load of the Kalman filter further reduced with the one-state modeling approach. By discarding one element, either the in-phase or the quadrature component from the two-dimensional measurement equation in (4), the state vector remains for estimation in any one of the two one-dimensional measurement equations, i.e.,

$$z_k^I=u_k^I\cos\theta_k-u_k^Q\sin\theta_k+v_k^I \tag{20}$$

or

$$z_k^Q=u_k^Q\cos\theta_k+u_k^I\sin\theta_k+v_k^Q. \tag{21}$$

From simulation results, the performance degradation due to the loss of certain observation information is not significant.

TABLE II. COMPARISON OF THE COMPUTATIONAL COMPLEXITY

	L_k	Σ_k	Ω_k^{-1}	H_k'	R_k	Q_k
Two-State Modeling	2x2	2x2	2x2	2x2	2x2	2x2
One-State Modeling	1x2	1x1	2x2	1x2	2x2	1x1
One-State Modeling with Reduced Observation	1x1	1x1	1x1	1x1	1x1	1x1

NOTATION:
L_k: Kalman gain matrix; $\sum_k$: Error covariance matrix
R_k , Q_k: Measurement noise matrix and process noise matrix
H_k' : Measurement matrix
$m \times n$: Matrix of dimension *m*-row by *n*-column
For a matrix of dimension 1×1, it is simply a scalar.

TABLE III. SPECIFICATION OF A CABLE DOWNSTREAM RECEIVER

Modulation	64-QAM@5 MBaud
Pulse Shaping Filter	A 41-tap SRRC filter with roll-off 0.18
Sampling Frequency	20 MSamples/sec
Center Frequency	600 MHz
Carrier Impairment	Carrier frequency offset=100 KHz
Timing Impairment	Sampling frequency offset=50 ppm
Adaptive Equalizer	24-tap feedforward FIR equalizer
Channel Model	Refer to Fig. 2 with AWGN, SNR=25 dB

D. Complexity of Kalman-Based Carrier Synchroniuzation

The computational complexity of the Kalman filter based on the two-state, one-state, and one-state with reduced observation modeling approaches is compared in Table II by analyzing the dimension of the involved matrices. The two-state modeling approach requires all computations based on matrices of dimension 2×2; on the other hand, the one-state modeling scheme reduces the number of matrices of dimension 2×2 to one-third of the original size with some being simplified to a scalar operation. Thus, the computational load of the Kalman filter can be effectively relieved by using the one-state modeling approach. Furthermore, with its measurement equation being reduced to one dimension, the matrix operation required by a Kalman filter can be completely removed.

IV. SIMULATION RESULTS

The application of the cable modem downstream system with the specification listed in Table III is used to demonstrate the proposed algorithm for adaptive carrier synchronization. The channel impulse response with 70 complex taps is shown in Fig. 2.

The system operates initially with the Godard's CMA blind equalization [18] by a T/2-spaced equalizer, where T is the symbol period. As the decision error rate is low enough, the blind mode then switches to the decision-directed (DD) mode to enhance performance. In the DD mode, the equalization adopts the least mean-square (LMS) algorithm with the reference signal provided by the QAM slicer output. The sample timing correction uses the cubic Lagrange interpolation filter [19] with the timing error signal generated by the Gardner's algorithm.

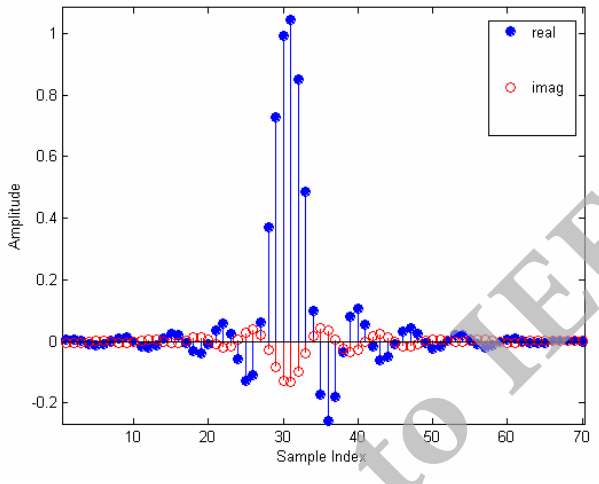

Figure 2. Channel impulse response.

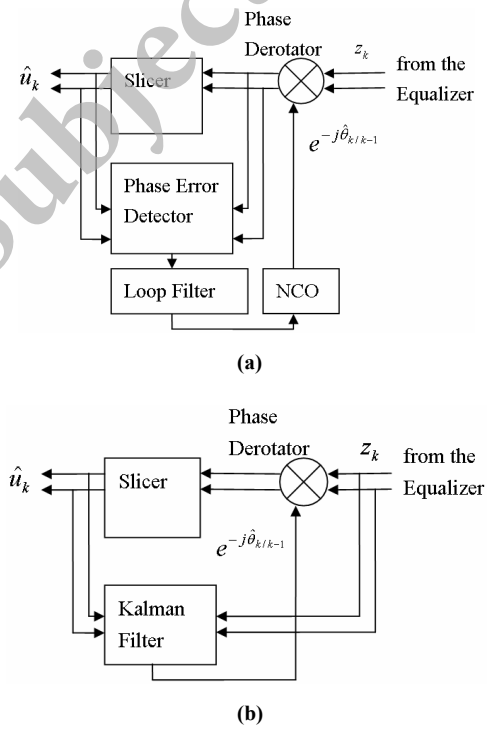

Figure 3. Carrier recovery loops: (a) PLL (b) the Kalman filter.

The carrier recovery structure uses either the conventional PLL or the Kalman filters as shown in Fig. 2. The carrier recovery schemes are simulated with the same system parameters for the performance comparison purpose.

Performance comparison of the proposed Kalman algorithm with $K_f = 2^{-11}$ and a conventional second-order PLL for carrier recovery is shown in Fig. 4. It can be seen that under the same steady-state performance, the proposed Kalman filter takes much less time to acquire a residual frequency offset than PLL. With 50 trials for both cases, the ensemble averages of carrier frequency offset estimation show that a much faster acquisition time of 2000T can be achieved by the Kalman filter than that by PLL. The parameter K_f determines the convergence rate and

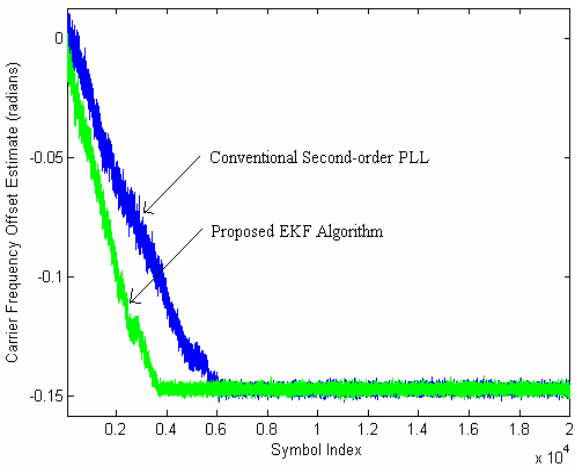

Figure 4. Comparison of the conventional second-order PLL and the proposed EKF algorithm for carrier frequency offset estimation.

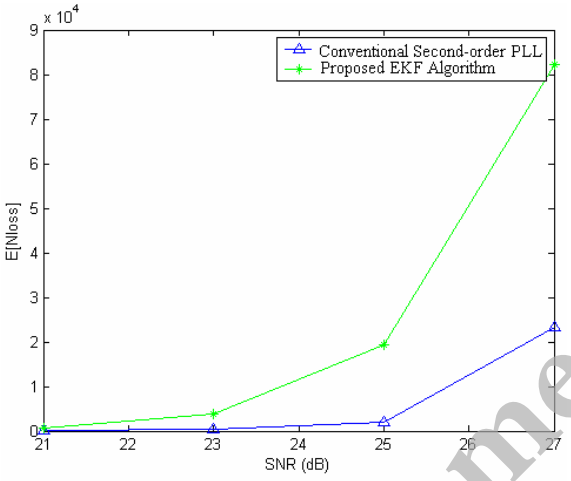

Figure 5. Comparison of MTLL.

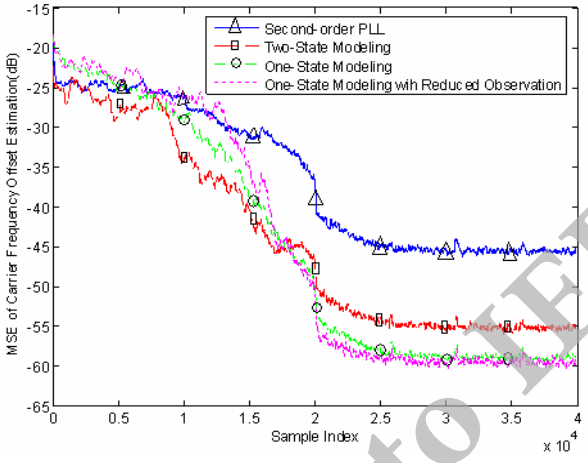

Figure 6. MSE comparison of carrier frequency offset estimation.

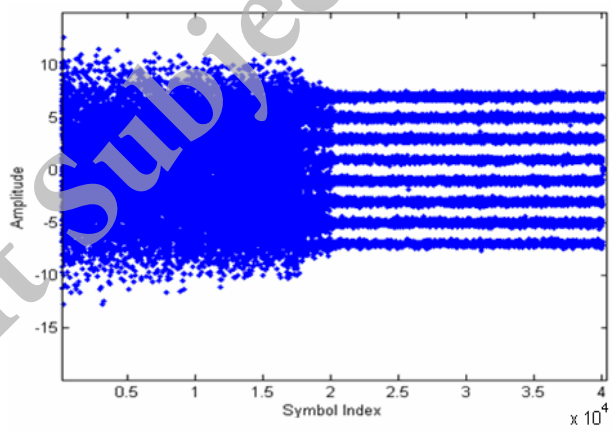

Figure 7. Constellation history of the in-phase signal.

$K_f = 2^{-10}$ can stably achieve a fast convergence within 2000 symbol iterations in this simulation environment.

The mean time to lose lock (MTLL) [20] with respect to PLL and the proposed Kalman filter for the CFO estimation error of -32 dB is shown in Fig. 5. Note that as the SNR increases, the Kalman filter has a much longer MTLL than PLL does.

Fig. 6 shows the mean squared error (MSE) of the estimated frequency offset for different carrier recovery algorithms with 50 ensemble averages. We choose the parameters to make all algorithms have the same convergence rate. The one-state modeling approaches have superior steady-state tracking performance and the reduced observation model makes little difference. It is interesting that the one-state model outperforms the conventional two-state model about 5 dB in this simulation. It can be explained as that the input frequency estimation equation in (12) is a better fit to practical situation than the frequency random model in (3).

The constellation history of the received in-phase signal after the phase derotator using the one-state modeling approach is plotted in Fig. 7. Note that the equalizer switches to the decision-directed mode at the 20000th symbol iteration, where the symbol levels can be significantly distinguished thereafter. With all transmission impairments including the channel effect, sampling frequency offset, and carrier frequency offset, the QAM constellation can reach a reasonably level in this simulation system.

V. Architecture and Design Verification

The functional blocks in Fig. 8 include main modules of the cable modem downstream system, where the square-root raised cosine (SRRC) filters are used as the pulse shaping filters with roll-off factor 0.18. By the fixed and symmetric properties of the filter coefficients, the number of multipliers needed for the SRRC filter can be reduced to half of the original size and the canonical signed digit (CSD) representation is used for a multiplier-less structure.

The timing recovery system includes the timing error detector (TED), a feedback control loop, and an interpolator with the Farrow structure to implement the digital-domain timing correction. The Gardner algorithm [21] is used to generate a timing error control signal

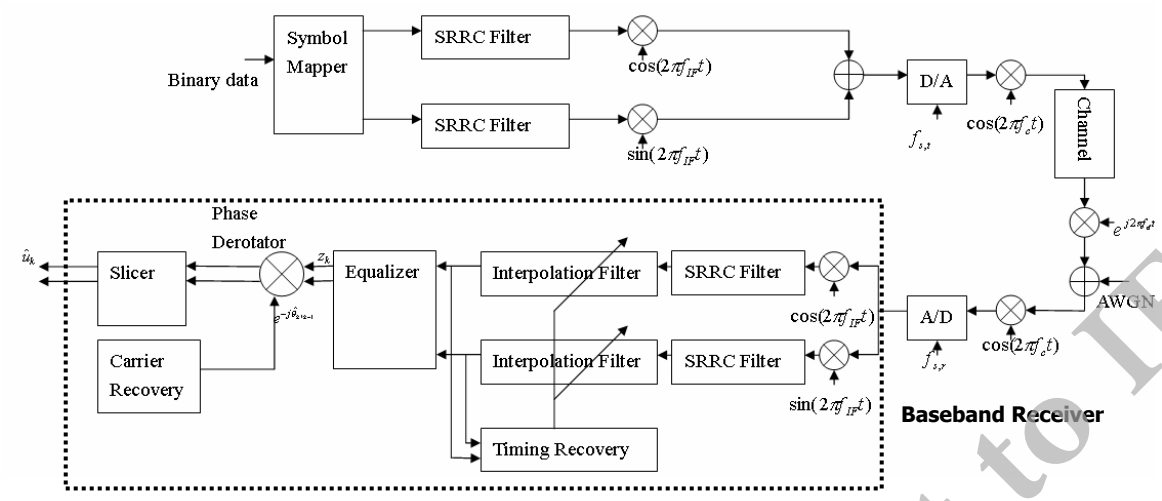

Fig. 8. Block diagram of the verified downstream receiver system.

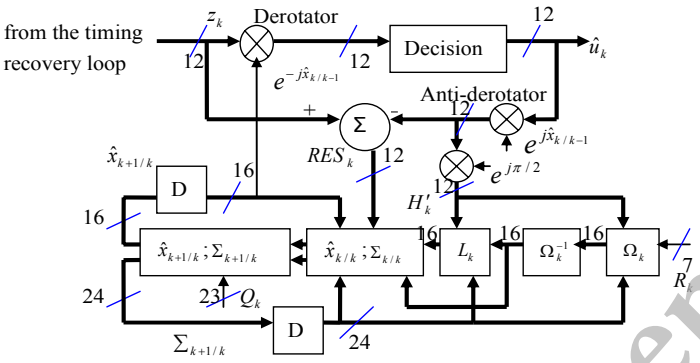

Figure 9. The carrier reocvery system applying the proposed algorithm.

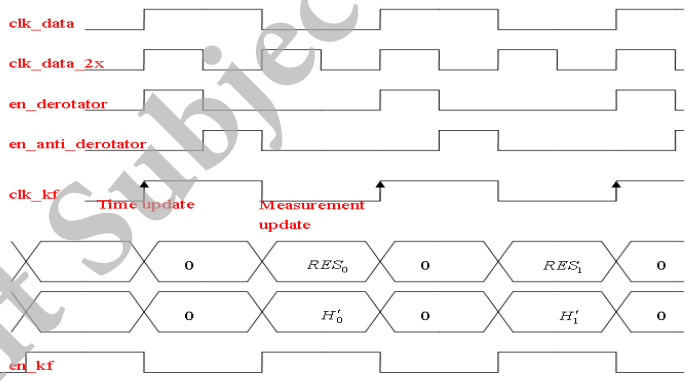

Figure 10. The timing diagram of the Kalman algorithm.

$$e(2k) = \mathrm{Re}\{z(2k)\cdot[z(2k+1) - z(2k-1)]^*\} \qquad (22)$$

where **Re{.}** denotes the real part, and $z(2k)$ represent the 2-to-1 downsample output of $y(k)$. In this system, the timing error signal in (22) is efficient for a robust operation. Hence, a first-order loop filter and a numerically controlled oscillator (NCO) work well to lock the control signal for the interpolator.

The architecture of the Kalman carrier recovery is depicted in Fig. 9. Main components include a phase derotator, an extended Kalman algorithm, and a hard decision device. The major cost is the complexity of matrix operations, specifically the calculation of Ω_k^{-1}. In the proposed two-state system six 2-by-2 matrices are required to be computed, while in the one-state system only scalar operations are required. The Kalman-based carrier recovery loop operates at the symbol rate. The timing sequence for the operation is shown in Fig. 10. The clock duty cycle is divided into two parts: the first half is used for the prediction stage and the second is used for the filtering stage.

To verify the hardware design, the testbed platform as shown in Fig. 11 is established with the VHDL design. The FPGA resource utilization report is listed in Table IV. As shown by the number of occupied slices, roughly half of the FPGA logic blocks remain available. Note that the design of blind equalizer is not included in the report since it occupies large circuit area and thus is allocated on another FPGA. The down-converted signal influenced by the timing and carrier impairments is fed as stimulus to the FPGA-prototyped system through a programmable data generator. Then the logic analyzer (LA) is used to grab the data of interest for analysis. Whenever triggered, the logic analysis system synchronously probes data from the prototype system. The digital in-phase and quadrature signals after processing are displayed on the LA scope screen as shown in Fig. 12.

VI. Conclusion

A new carrier recovery scheme applying the extended Kalman filtering algorithm with reduced computational complexity is proposed. We have shown that the proposed algorithm is able to be integrated with blind equalization, timing recovery, and the decision-aided feedback in a practical cable modem downstream receiver. Additionally, the proposed carrier recovery algorithm better compromises the steady-state performance and the acquisition time by an automatically adjusted loop bandwidth in MMSE sense compared to the conventional PLL.

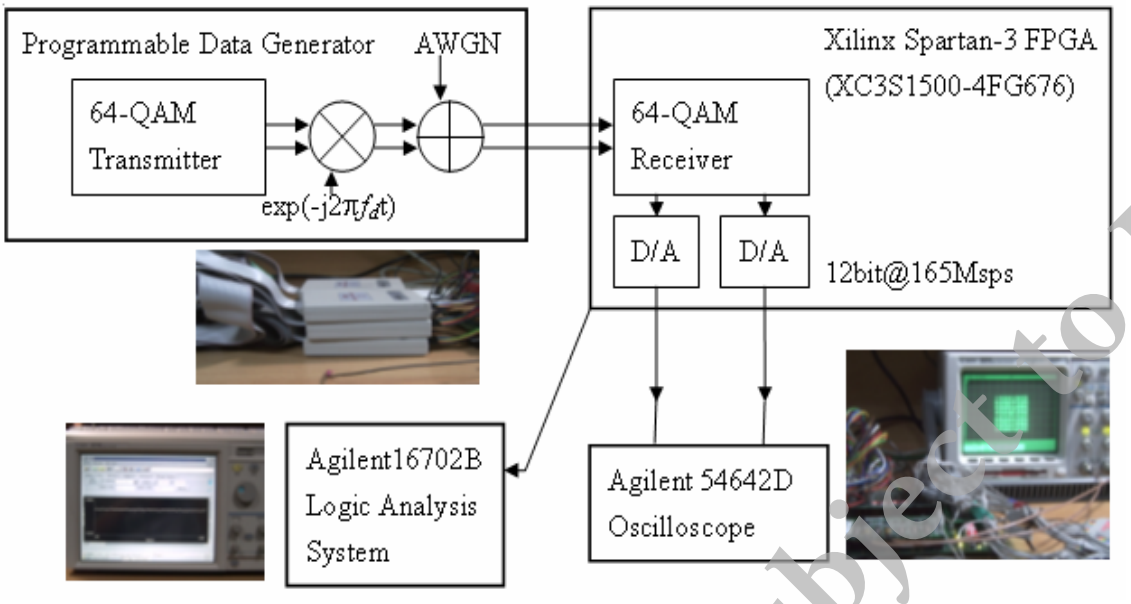

Fig. 11. Testbed platform for verification.

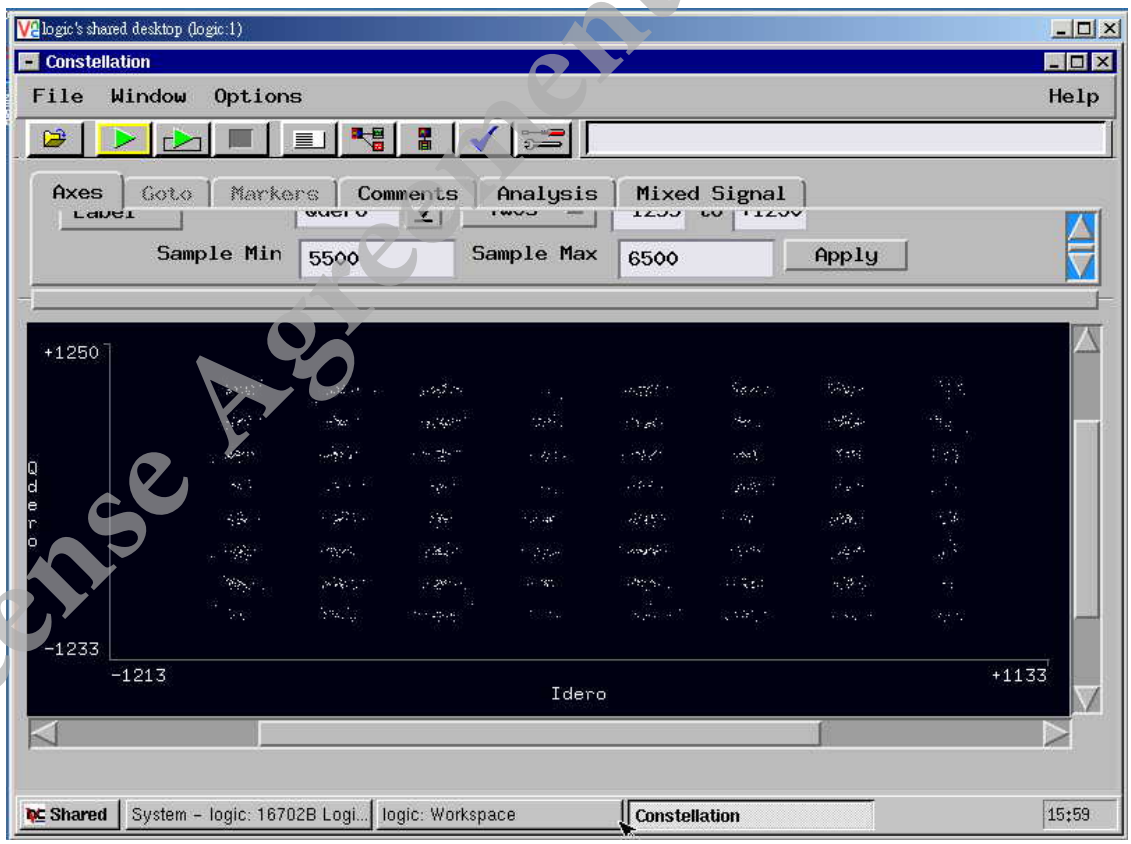

Fig. 12. Receiver I/Q signal constellation with carrier recovery on LA scope.

TABLE IV. DESIGN SUMMARY OF FPGA* (ISE XST SYNTHESIZER)

Item	Used	Total	Usage (%)
Sequential Logic Utilization	1,680	2,6624	6
Combinatorial Logic Utilization	8,332	2,6624	31
Logic Distribution (Slices)	5,908	1,3312	44
Maximum Frequency	73.6 MHz		

*Xilinx Spartan-3 FPGA (XC3S1500-4FG676)

REFERENCES

[1] L. K. Tan et al., "A 70-Mb/s variable-rate 1024-QAM cable receiver IC with integrated 10-b ADC and FEC decoder," *IEEE Journal of Solid State Circuits*, Vol. 33, No. 12, pp. 2205-2218, Dec. 1998.

[2] D. A. Byan, "QAM for terrestrial and cable transmission," *IEEE Transactions on Consumer Electronics*, Vol. 41, No. 3, pp.383-391, Aug. 1995.

[3] C. H. Huang, S. C. Chen, and D. C. Chang, "A study on joint effect of synchronization and channel estimation in the DVB-T receiver," in 2005 8th *International Symposium on Communications (ISCOM 2005)*, Kaoshiung, Taiwan, Nov. 2005.

[4] D. R. Stephens, *Phase-locked Loops for Wireless Communications: Digital, Analog and Optical Implementations*, Kluwer Academic Publishers, 2nd ed., 2002.

[5] L. Erup, F. M. Gardner, and R. A. Harris, "Interpolation in digital modems — part II: Implementation and performance," *IEEE Transactions on Communications*, Vol. 41, No. 6, pp. 998-1008, June 1993.

[6] J. Tian, B. Shen, A. Li, J. Su, and Q. Zhang, "Joint carrier recovery and adaptive equalization for high-order QAM," in *IEEE International Symposium on Circuits and Systems* (*ISCAS 2005*), Vol. 2, May 2005, pp. 928-931.

[7] Y. Ouyang, and C. L. Wang, "A new carrier recovery loop for high-order quadrature amplitude modulation," in *IEEE Global Telecommunications Conference* (*GLOBECOM'02*), Vol. 1, Nov. 2002, pp.478-482.

[8] K. Y. Kim and H. J. Choi, "Design of carrier recovery algorithm for high-order QAM with large frequency acquisition range," in *IEEE International Conference on Communications* (*ICC 2001*), Vol. 4, June 2001, pp. 1016-1020.

[9] C. N. Ke, C. Y. Huang, and C. P. Fan, "An adaptive carrier synchronizer for M-QAM cable receiver," *IEEE Transactions on Consumer Electronics*, Vol. 49, No. 4, pp. 983-989, Nov. 2003.

[10] Z. Hang and M. Renfors, "A new symbol synchronizer with reduced timing jitter for QAM systems," in *IEEE Global Telecommunications Conference* (*GLOBECOM'95*), Vol. 2, Nov. 1995, pp. 1292-1296.

[11] A. Patapoutian, "Application of Kalman filters with a loop delay in synchronization," *IEEE Transactions on Communications*, Vol. 50, No. 5, pp. 703-706, May 2002.

[12] A. Aghamohammadi, H. Meyr, and G. Ascheid, "Adaptive synchronization and channel parameter estimation using an extended Kalman filter," *IEEE Transactions on Communications*, Vol. 37, pp. 1212-1219, Nov. 1989.

[13] T. Oren and D. Raphaeli, "A new suppressed carrier synchronizer with reduced phase jitter for QAM systems," in *The 21th IEEE Convention of Electrical and Electroni Engineers in Israel*, April 2000, pp. 443-447.

[14] G. Skiller and D. Huang, "The stationary phase error distribution of a digital phase-lock loop," *IEEE Transactions on Communications*, Vol. 48, No. 6, pp. 925-927, June 2000.

[15] H. Jin et al., "Carrier phase and frequency recovery for MIMO-OFDM," in *IEEE Global Telecommunications Conference* (*GLOBECOM 2004*, 2004), pp. 2669-2674.

[16] F. D. Nunes and J. M. Leitao, "State-space estimation of rapidly-varying carrier frequency offsets in OFDM systems," in *2003 4th IEEE Workshop on Signal Processing Advances in Wireless Communications*, 2003, pp. 585-589.

[17] B. D. O. Anderson and J. B. Moore, *Optimal Filtering*, Englewood Cliffs, New Jersey: Prentice-Hall, 1979.

[18] D. N. Godard, "Self-recovering equalizer and carrier tracking in two dimensional data communication system," *IEEE Transactions on Communications*, Vol. 28, No. 11, pp. 1867-1875, Nov. 1980.

[19] F. M. Gardner, "Interpolation in digital modems—part I: Fundamentals," *IEEE Transactions on Communications*, Vol. 41, No. 3, pp. 501-507, March 1993.

[20] L. Brecher, N. Sommer, and E. Weinstein, "Analysis of lock-loss events in discrete-time phase locked loop (PLL)," in *Proceeding of the 11th IEEE International Conference on Electronics*, Dec. 2004, pp.354-357.

[21] F. M. Gardner, "A BPSK/QPSK timing-error detector for sampled receiver," *IEEE Transactions on Communications*, Vol. 34, No. 5, pp. 423-429, May 1986.

Wei-Tsen Lin received the M. S. degree in communication engineering from the National Central University, Taoyuang, Taiwan in 2005. He is now working at Mediatek Inc., Hsinchu, Taiwan in broadband wireless communication IC fields. He majors in adaptive signal processing, VLSI design, and communication baseband architecture design.

Dah-Chung Chang (M'94) received the the M.S. and Ph.D. degrees in electrical engineering from the National Chiao Tung University, Hsinchu, Taiwan in 1993 and 1998, respectively. From Oct. 1998 to Jan. 2003, he worked in Computer and Communications Research Laboratories at Industrial Technology Research Institute, Hsinchu, Taiwan. In Feb. 2003, he joined the faculty of the department of communication engineering at National Central University, Taoyuang, Taiwan. His research interests include digital transceiver architecture design, OFDM, and adaptive signal processing and applications.